particles

Article

Diquarks and Λ^0/π^+, Ξ^-/π^+ Ratios in the Framework of the EPNJL Model

Alexandra Friesen * and Yuriy Kalinovsky

Joint Institute for Nuclear Research, 141980 Dubna, Russia; kalinov@jinr.ru
* Correspondence: avfriesen@theor.jinr.ru

Abstract: The applicability of the effective models to the description of baryons and the behaviour of ratios of strange baryons to pions is discussed. In the framework of the EPNJL model, the Bethe–Salpeter equation is used to find masses of baryons, which are considered to be in a diquark-quark state. Baryon melting is discussed at a finite chemical potential, and a flavor dependence of the hadronic deconfinement temperature is pointed out. It is shown that the description of the diquark-quark state at finite chemical potential is limited due to the occurrence of Bose condensate. This effect is strongly manifested in the description of light diquarks and baryons. Both the Λ^0/π^+ and Ξ^-/π^+ ratios show a sharp behaviour as functions of the T/μ_B variable, where T and μ_B are calculated along the melting lines.

Keywords: PNJL model; baryon structure; diquark-quark bounding state; hadronic deconfinement; baryon-to-meson ratio

check for updates

Citation: Friesen, A.; Kalinovsky, Y. Diquarks and Λ^0/π^+, Ξ^-/π^+ Ratios in the Framework of the EPNJL Model. *Particles* **2023**, *6*, 876–885. https://doi.org/10.3390/particles6040056

Academic Editor: Armen Sedrakian

Received: 14 August 2023
Revised: 13 September 2023
Accepted: 21 September 2023
Published: 10 October 2023

Copyright: © 2023 by the authors. Licensee MDPI, Basel, Switzerland. This article is an open access article distributed under the terms and conditions of the Creative Commons Attribution (CC BY) license (https://creativecommons.org/licenses/by/4.0/).

1. Introduction

In our previous works [1–4], the peak-like structure in a K^+/π^+ ratio was discussed in the framework of the Polyakov loop extended Nambu–Jona–Lasinio model (PNJL) as well as its modifications, including the vector interaction. The interest in this structure is due to the search for signals of a phase transition from the hadron phase to the quark-gluon plasma (QGP) formation during a heavy ion collision [5,6]. The quick rise in the K^+/π^+ ratio is associated with the phase transition in the medium, while the jump from the maximum value to the constant valley is explained as the QGP formation during the collision. This is a consequence of the fact that after the deconfinement transition occurs in the system, the strangeness yield becomes independent of the collision energy [7–10]. Recent investigations showed that the K^+/π^+ peak strongly depends on the volume of the system and tends to be less pronounced in small-sized systems [7,11].

The meson-to-meson ratios are widely considered both in theoretical and experimental works, in contrast to the baryon-to-meson ratios, although they also have a peak-like structure. In [12], in the framework of the thermal model, it was shown that unlike the K^+/π^+-ratio, the peak for Λ^0/π^+ does not disappear with reducing the system size.

The choice of the (E)PNJL model for such investigations is conditioned by the possibility to describe within the model both the chiral phase transition and the deconfinement transition, which can give a hint for understanding the nature of the peaks at least quantitatively. For the next step, it is interesting to consider the baryon-to-meson ratios in the framework of the model. The controversy of the applicability and complexity of this task is related to the problem of describing baryons in the frame of NJL-like models. The most detailed and exact description of baryons requires solving the three-body Faddeev equation, which leads to considering baryons as a bound state of a quark and diquark [13,14]. The so-called "static approximation" of the Faddeev equation leads to the Bethe–Salpeter equation, which is based on the polarisation loop in the diquark-quark scattering channel [15]. But the diquark-quark structure of baryons leads to the non-obvious nature of the description of baryons in a dense medium, where the formation of a Bose condensate occurs and the diquark states melt.

The results of our calculations and discussion about aspects of applicability of the model are presented in Section 5.

2. SU(3) PNJL Lagrangian

The complete Lagrangian of the SU(3) PNJL model with the vector interaction and $U_A(1)$ anomaly has the following form [15,16]:

$$\begin{aligned}
\mathcal{L} &= \bar{q}\,(\,i\,\gamma^{\mu}\,D_{\mu}\,-\,\hat{m}-\gamma_0\mu)\,q \\
&+ \tfrac{1}{2}\,g_S\,\textstyle\sum_{a=0}^{8}\,[\,(\,\bar{q}\,\lambda^{a}\,q\,)^2\,+\,(\,\bar{q}\,i\,\gamma_5\,\lambda^{a}\,q\,)^2\,] \\
&- \tfrac{1}{2}g_{\mathrm{V}}\textstyle\sum_{a=0}^{8}\,[(\bar{q}\gamma_{\mu}\lambda^{a}q)^2+(\bar{q}\gamma_{\mu}i\gamma_5\lambda^{a}q)^2] \\
&- \textstyle\sum_{\alpha}g^{\alpha}_{\mathrm{diq}}\sum_{i,j}(\bar{q}_a\Gamma^{i}_{\alpha}q^{C}_b)\left(\bar{q}^{C}_d\Gamma^{j}_{\alpha}q_e\right)\varepsilon^{abc}\varepsilon^{de}_{c} \\
&+ \mathcal{L}_{\mathrm{det}}-\mathcal{U}(\Phi,\bar{\Phi};T),
\end{aligned} \tag{1}$$

where $q=(u,d,s)$ is the quark field with three flavours, q^{C} is the charge-conjugated quark field, $\hat{m}=\mathrm{diag}(m_u,m_d,m_s)$ is the current quark mass matrix, and g_{S} and g_{V}, g_{diq} are the coupling constants. The entanglement PNJL model (EPNJL) includes the constants $g_{\mathrm{S}}, g_{\mathrm{V}}$ introduced as functions of T to enhance the coupling between quarks and the gauge field [2,17]. Γ^{j}_{α} is a product of the Dirac matrices γ^{μ} and Gell-Mann matrices λ^{α}, where the index α describes the type of diquarks. The covariant derivative is $\mathrm{D}_{\mu}=\partial^{\mu}-iA^{\mu}$, where A^{μ} is the gauge field with $A^{0}=-iA_4$ and $A^{\mu}(x)=g_S A^{\mu}_{a}\frac{\lambda_a}{2}$ absorbs the strong interaction coupling. The Kobayashi–Masakawa–t'Hooft (KMT) interaction is described by the term

$$\mathcal{L}_{\mathrm{det}}=g_D\,\{\det[\bar{q}\,(\,1\,+\,\gamma_5\,)\,q\,]+\det[\bar{q}\,(\,1\,-\,\gamma_5\,)\,q\,]\,\}$$

The last term is the effective potential $\mathcal{U}(\Phi,\bar{\Phi};T)$, expressed in terms of the traced Polyakov loop $\Phi=N_c^{-1}\mathrm{tr}_c\langle L(\bar{x})\rangle$ [18], where

$$L(\bar{x})=\mathcal{P}\mathrm{exp}\left[\int_0^{\infty}d\tau A_4(\bar{x},\tau)\right]. \tag{2}$$

The effective potential describes the confinement properties (Z_3 symmetry) and is constructed on the basis of Lattice inputs in the pure gauge sector. In this work, we use the standard polynomial form of the effective potential [4,15]. The effect of the vector interaction on the position of the critical end point in the phase diagram and on the behaviour of the peak in the K^{+}/π^{+} ratio was discussed in previous works [1–4].

The grand potential density $\Omega(T,\mu_i)$ in the mean-field approximation with $g_{\mathrm{V}}=0$ can be obtained from the Lagrangian density (Equation (1)) and leads to a set of self-consistent equations:

$$\frac{\partial\Omega}{\partial\langle\bar{q}_i q_i\rangle}=0,\;\;\frac{\partial\Omega}{\partial\Phi}=0,\;\;\frac{\partial\Omega}{\partial\bar{\Phi}}=0, \tag{3}$$

where $\Phi,\bar{\Phi}$ are the Polyakov fields. The gap equations for the quark masses are

$$m_i = m_{0i}-2g_S\langle\bar{q}_i q_i\rangle-2g_D\langle\bar{q}_j q_j\rangle\langle\bar{q}_k q_k\rangle, \tag{4}$$

where $i,j,k=u,d,s$ are chosen in cyclic order, m_i represents the constituent quark masses, and the quark condensates are

$$\langle\bar{q}_i q_i\rangle = -2N_c\int\frac{d^3p}{(2\pi)^3}\frac{m_i}{E_i}(1-f^{+}_{\Phi}(E_i)-f^{-}_{\Phi}(E_i)) \tag{5}$$

with modified Fermi functions $f^{\pm}_{\Phi}(E_i)$:

$$f^{+}_{\Phi}(E_f) = \frac{(\bar{\Phi} + 2\Phi Y)Y + Y^3}{1 + 3(\bar{\Phi} + \Phi Y)Y + Y^3}, \tag{6}$$

$$f^{-}_{\Phi}(E_f) = \frac{(\Phi + 2\bar{\Phi}\bar{Y})\bar{Y} + \bar{Y}^3}{1 + 3(\Phi + \bar{\Phi}\bar{Y})\bar{Y} + \bar{Y}^3}, \tag{7}$$

where $Y = \mathrm{e}^{-(E_i - \mu_f)/T}$ and $\bar{Y} = \mathrm{e}^{-(E_i + \tilde{\mu}_i)/T}$.

3. Mass Equations for Standard Particles

To describe mesons and diquarks as quark-antiquark and quark-quark bound states, the random-phase approximation is usually used in the framework of the (E)PNJL model. The masses of bound states are defined by the polarisation function Π_{ij}.

Mesons as a quark-antiquark system have the polarisation loop shown in Figure 1. The polarisation function for mesons is defined as

$$\Pi_{ij} = \int \frac{dp}{(2\pi)^4} \mathrm{tr}\{S^i(\hat{q}_i, m_i)\Gamma_j S^j(\hat{q}_j, m_j)\Gamma_i\}, \tag{8}$$

where $\Gamma_{i,j}$ represents the vertex matrices (Figure 2) and $S^i(\hat{q}_i, m_i) = (\hat{q}_i + \gamma_0(\mu_i - iA_4) - m_i)^{-1}$ is the $i-$ flavour quark propagator. The meson mass is obtained from the Bethe–Salpeter equation in the meson rest frame ($\bar{P} = 0$):

$$1 - P_{ij}\Pi_{ij}(P_0 = M, \bar{P} = 0) = 0, \tag{9}$$

where the function P_{ij} depends on the type of meson (see the details in [19]), such as for the pion, which is a pseudoscalar meson $P_{ud} = g_S + g_D\langle\bar{q}_s q_s\rangle$.

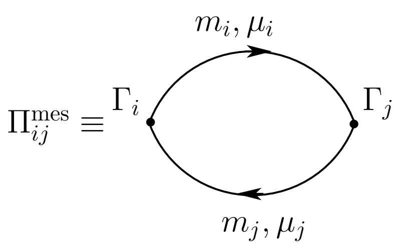

Figure 1. Polarisation loop for mesons.

Diquarks are considered as two-quark systems, and to describe the polarisation loop in the same way, the "antiquark" is replaced by its charge conjugate propagator. Then, two diagrams should be taken into account, but it can be shown that they give the same result. Polarisation loops for diquarks are shown in Figure 2, where $\mathcal{C} = i\gamma_0\gamma_2$ is the charge conjugation operator and $\Gamma_{i,j}$ represents the vertex functions.

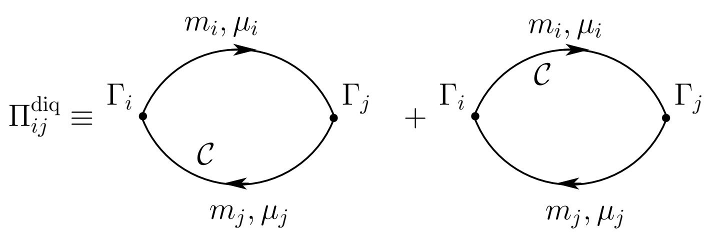

Figure 2. Polarisation loops for diquarks, where "$\mathcal{C}$" is the charge conjugation operator.

According to group theory, diquarks can be represented by symmetric and antisymmetric wave functions both in colour and flavour spaces. Since diquarks are used to construct baryons which are "white objects", only diquarks with a colour-antisymmetric wave function are considered. According to the interaction type, diquarks can be of scalar, pseudo-scalar, axial, and vectorial types, following the rule that the diquark wave function is totally antisymmetric (see Table 1).

Table 1. List of mesons and diquarks.

Γ	Meson Type	Possible Mesons	Diquark Type	Possible Diquarks
$i\gamma_5$	pseudoscalar	π, K	scalar	
1	scalar	σ, K_0^*	pseudoscalar	(ud), (us), (ds)
$\gamma^\mu i\gamma_5$	axial-vector	a_1^*, K_1^*	vector	
$i\gamma^\mu$	vector	ρ, K^*	axial-vector	$[ud]$, $[us]$, $[ds]$, $[uu]$, $[dd]$, $[ss]$

The Bethe–Salpeter equation for diquarks in the rest frame is

$$1 - Z_{\text{diq}}\Pi_{ij}(P_0 = M_{\text{diq}}, \bar{P} = 0) = 0, \tag{10}$$

with polarisation operators corresponding to Figure 2:

$$\Pi_{ij}^{(1)} = \int \frac{dp}{(2\pi)^4} tr\{S^i(\hat{q}_i, m_i)\Gamma_j S^{jC}(\hat{q}_j, m_j)\Gamma_i\}, \tag{11}$$

$$\Pi_{ij}^{(2)} = \int \frac{dp}{(2\pi)^4} tr\{S^{iC}(\hat{q}_i, m_i)\Gamma_j S^{j}(\hat{q}_j, m_j)\Gamma_i\}, \tag{12}$$

which give the same result, where $S^{iC}(\hat{q}_i) = (\hat{q}_i - \gamma_0(\mu_i + iA_4) - m_i)^{-1}$ is the propagator of the charge conjugated quark and Z_{diq} is the coupling constant for diquarks, yielding $Z_{\text{diq}} = g^s_{\text{diq}}$ for scalar and pseudoscalar diquarks and $Z_{\text{diq}} = g^s_{\text{diq}}/4$ for vector and axial-vector diquarks. According to the Lagrangian equation (Equation (1)) and the Fierz transformation, the coupling constant g^s_{diq} is referred to g_S as $g^s_{\text{diq}} = 3g_S/4$ and is usually chosen such that $g^s_{\text{diq}} \sim (0.705 - 0.75)g_S$ [15,16].

The description of baryons is a more complicated task, since they are complex structures of three quarks coupled through the exchange of gluons. Thus, the modelling of a three-body system is required, and the Faddeev equation has to be considered. However, some simplifications of the Faddeev equation allow one to consider the baryon as a diquark-quark bound state [13–16]. Considering the static approximation for the four-point interaction leads to the loop structure of the transition matrix and a matrix Bethe–Salpeter-like equation for the baryon mass:

$$1 - \Pi_{i(D)}(k_0, \vec{k}) \cdot Z_{ij} = 0, \tag{13}$$

where the constant Z_{ij} is defined as

$$Z_{ij} = \frac{g_{ik} g_{jk}}{m_k}, \tag{14}$$

where g_{ij} is the diquark-quark coupling $D_{ij} \to q_i q_j$ and g_{ud} includes the factor (-2) [15]. The baryon loop function is shown in the Figure3, where double line corresponds to the diquark and simple line is quark line.

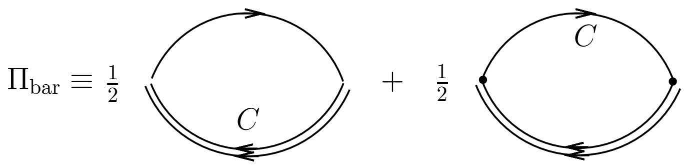

Figure 3. The baryon loop function.

Just as for diquarks, two quark-diquark loops should be taken into account, and it can easily be shown that they give the same results [15]:

$$\Pi^{(1)}_{i(D)} = \int \frac{dp}{(2\pi)^4} tr\{S^i(\hat{q}_i, m_i)\Gamma_j S^{jC}_D(\hat{q}_j, m_j)\Gamma_i\}, \tag{15}$$

$$\Pi^{(2)}_{i(D)} = \int \frac{dp}{(2\pi)^4} tr\{S^{iC}(\hat{q}_i, m_i)\Gamma_j S^{j}_D(\hat{q}_j, m_j)\Gamma_i\}. \tag{16}$$

It should be noted here that the axial-diquark contribution to the members of the baryon octet is neglected [15,20].

4. Numerical Results

In previous works [1–3], a detailed study of K/π ratios was carried out in the framework of PNJL-like models. As the collision energy $\sqrt{s_{\mathrm{NN}}}$ never appears in effective models, a trick with fitting $\sqrt{s_{\mathrm{NN}}}$ with the pair (T, μ_B) from the statistical model was used. In the statistical model, the temperature and the baryon chemical potential of freeze-out are assigned to each collision energy (e.g., as suggested by Cleymans et al. [12]). Supposing that the chiral phase transition line in the EPNJL model corresponds to the freeze-out, the K$/\pi$ ratio can be considered as a function of a new variable T/μ_B instead of $\sqrt{s_{\mathrm{NN}}}$, where (T, μ_B) are taken along the phase transition line.

The phase diagram has a classic structure with smooth crossover at low chemical potentials and the first-order chiral phase transition at a high chemical potential. The PNJL model has a crossover temperature ($T_c = 0.27$ GeV) higher than the Lattice prediction ($T_c \sim 0.17$ GeV). An extended version of the PNJL model (EPNJL) with $f_V(T)$, $g_S(T)$ was introduced to reduce the critical temperature of the crossover to a lower value of $T_c^{\mathrm{EPNJL}} = 0.18$ GeV due to enhanced interaction between the quarks and gauge sector [4]. For more detailed study, the meson masses were calculated with both the Bethe–Salpeter and Beth–Uhlenbeck approaches. The latter is preferable for considering mesons in hot and dense matter, since it takes into account their spectral functions and correlations.

For the effective models, the ratio of the particle number can be calculated in terms of the ratio of the number densities:

$$n = d\int_0^\infty p^2 dp \frac{1}{e^{\beta(\sqrt{p^2+m^2} \mp \mu)} \pm 1}, \tag{17}$$

where d is the corresponding degeneracy factor, the upper sign in the denominator refers to fermions, the lower sign refers to bosons, and $\beta = T^{-1}$. The pion chemical potential is a phenomenological parameter, and it was chosen to be constant. The baryon chemical potential is calculated as the sum of the chemical potentials of constituent quarks. The degeneracy factors are calculated as $(2s+1)(2I+1)$ since Λ^0 is two, and for Ξ^-, it is four.

Figure 4 shows contour graphs for the K^+/π^+ and K^-/π^- ratios obtained with the Beth–Uhlenbeck approach of the EPNJL model with $g_V = 0.6 g_S$ [3]. The black lines show the phase transition (crossover) lines. It can be seen that when shifting along the phase transition line from low to high temperatures, the trajectory shows a quick enhancement and then a fall for K^+/π^+ and a smooth increase for K^-/π^-.

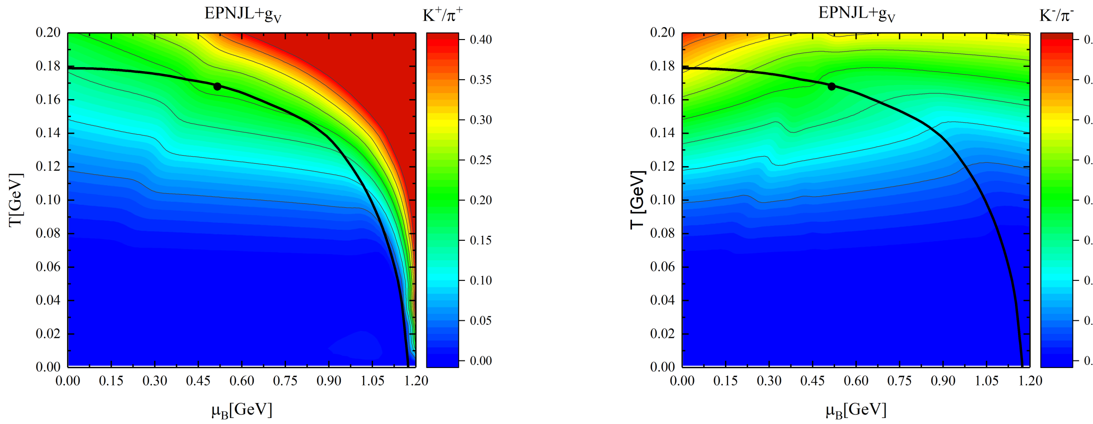

Figure 4. K^+/π^+ (**left**) and K^-/π^- (**right**) on the $T - \mu_B$ plane for the EPNJL model with $g_V = 0.6g_S$ (no CEP) and $\mu_\pi = 0.147$ GeV. The black dot indicates the maximum of K^+/π^+ ratio on the line of pseudo-critical temperatures for the chiral transition (our proxy for chemical freeze-out).

The results in Figure 4 are presented for the case with a fixed pion chemical potential of $\mu_\pi = 0.147.6$ GeV. In order to reproduce the experimental data, the dependence of the pion and the strange quark chemical potentials on the variable $x = T/\mu_B$ should be introduced. The expressions should describe the increase in the pion chemical potential with x and the decrease in the strange quark chemical potential. For their x dependence, the functions of the Woods–Saxon form are suggested [2]:

$$\mu_\pi(x) = \mu_\pi^{\text{min}} + \frac{\mu_\pi^{\text{max}} - \mu_\pi^{\text{min}}}{1 + \exp(-(x - x_\pi^{\text{th}})/\Delta x_\pi)}, \tag{18}$$

$$\mu_s(x) = \frac{\mu_s^{\text{max}}}{1 + \exp(-(x - x_s^{\text{th}})/\Delta x_s)}. \tag{19}$$

The parameters in Equations (18) and (19) were obtained from fitting the experimental data (see for details [2,3]). The best parameter values for the EPNJL model are $\mu_\pi^{\text{max}} = 107 \pm 10$ MeV, $\mu_\pi^{\text{min}} = 92$ MeV, $x_\pi^{\text{th}} = 0.409$, and $\Delta x_\pi = 0.00685$. And for μ_s, the parameter values are $\mu_s^{\text{max}}/\mu_u^{\text{crit}} = 0.205$, $x_s^{\text{th}} = 0.223$, and $\Delta x_s = 0.06$.

In the left panel of Figure 5, K^+/π^+ (black lines) and K^-/π^- (red lines) are shown as functions of T/μ_B obtained in the Beth–Uhlenbeck approach for the EPNJL model with $g_V = 0$ and μ_s and μ_π calculated according to Equations (18) and (19). Thin lines correspond to the case where $\mu_s = 0$ and a fixed μ_π. The shaded region corresponds to the error band due to normalisation to high x RHIC and LHC data. The behaviour of the potentials is shown in the right panel of Figure 5.

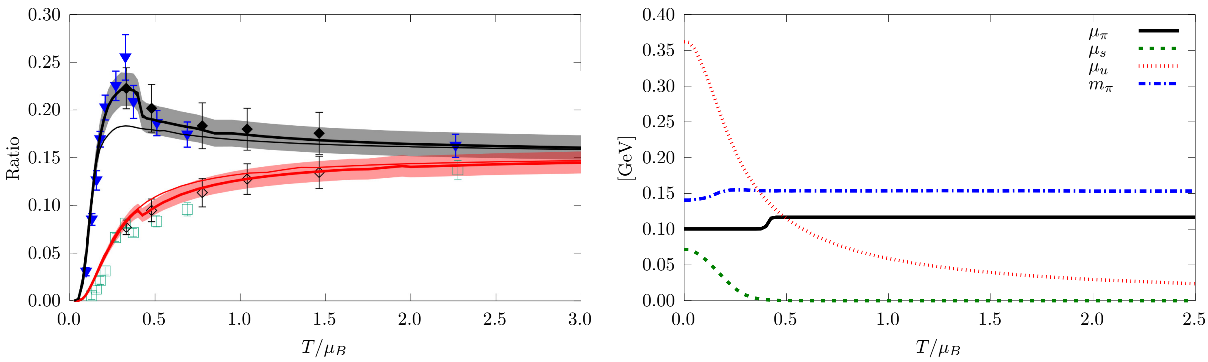

Figure 5. (**left**) The K^+/π^+ (black lines) and K^-/π^- (red lines) ratios are shown as a function of T/μ_B. Thin lines correspond to the case where $\mu_s = 0$ and fixed $\mu_\pi = 0.147$ GeV. (**right**) Chemical potentials and pion mass as functions of T/μ_B.

Figures 4 and 5 demonstrate that the "horn" structure in the K^+/π^+ ratio is less sensitive to the structure of the phase diagram and more sensitive to the properties of the medium. At $g_\mathrm{V} = 0.6 g_\mathrm{S}$, the phase diagram has a smooth crossover transition at a high density instead of the first-order transition when $g_\mathrm{V} = 0$. Nevertheless, the ratio keeps a "horn" structure. Changing the matter properties by modelling the chemical potentials for the pions and s-quark leads to the possibility of reproducing the experimental data.

The present work is devoted to the description of baryons and Ξ^-/π, Λ^0/π ratios within this kind of model. According to Equation (13), the Bethe–Salpeter equation for barions has a matrix form $\det(1 - Z\Pi) = 0$ where for Λ, we have

$$\Pi^\Lambda = \begin{bmatrix} \Pi_{(ds)u} & 0 & 0 \\ 0 & \Pi_{(us)d} & 0 \\ 0 & 0 & \Pi_{(ud)s} \end{bmatrix}, \qquad Z^\Lambda = \begin{bmatrix} 0 & Z_{ud} & Z_{us} \\ Z_{du} & 0 & Z_{ds} \\ Z_{su} & Z_{sd} & 0 \end{bmatrix}$$

and for Ξ, we have

$$\Pi^\Xi = \Pi_{(us)s}, \qquad Z^\Xi = Z_{ds}, \tag{20}$$

where functions Π and Z are presented in Equations (14)–(16).

The calculations were performed with the parameter set $m_{u0} = m_{d0} = 4.75$ MeV, $m_{s0} = 0.147$ GeV, $\Lambda = 0.708$ GeV, $g_S\Lambda^2 = 1.922$, $g_D\Lambda^5 = 10.0$, $g_\mathrm{V} = 0$, and $g_\mathrm{diq} = 0.725 g_\mathrm{S}$. The choice of the parameter set was driven by the requirement to have the proton and Λ masses below the threshold $M_D + m_q$.

The dissociation temperature for baryons is postulated from their diquark-quark structure. The Mott temperature ($T^\mathrm{bar}_\mathrm{Mott}$) is a temperature for which the mass of baryons is equal to the sum of the quark and diquark masses [15,20,21]. To avoid the situation where the diquark melts at a lower temperature and the baryon still exists, the baryon deconfinement temperature is chosen to be

$$T^\mathrm{bar}_\mathrm{dec} = \min\{T^\mathrm{bar}_\mathrm{Mott}, T^\mathrm{diq}_\mathrm{Mott}\}.$$

Nevertheless, even if the diquark already becomes unbound due to the Mott effect, the baryon can still be bound as a three-particle state (the so-called "borromean state") [21,22]. In this case, the "dissociation" temperature for baryons should be considered as the temperature when the baryon melts into three quarks (T_diss).

The dissociation boundaries of baryons corresponding to $\{T^\mathrm{bar}_\mathrm{dec}, T_\mathrm{diss}\}$ are shown in Figure 6 (right panel), with the light blue shaded area for Λ and the light green one for Ξ. The red line corresponds to the phase diagram of the EPNJL model with $g_\mathrm{V} = 0$. The dashed line corresponds to the crossover, and the solid line corresponds to the first-order transition. As can be seen in Figure 6, the Ξ^- baryon is described until $\mu_q \sim 0.37$ GeV, which is higher than $\mu_q \sim 0.27$ GeV for Λ. It appears that Ξ^- is considered a combination of the scalar (ds) diquark and s-quark, unlike Λ, which is a superposition of $(ud) + s$ and $(ds) + u$ ($(us) + d$) states. The diquark with a heavy quark survives at higher values of the chemical potential than light diquarks. The left panel of Figure 6 shows the masses of diquarks (dashed), baryons (solid), and their thresholds $M_D + m_q$ (short-dashed) as functions of the chemical potential μ_q. Light diquarks melt at lower densities (or chemical potentials) due to the origin of the Bose–Einstein condensate.

The results for the baryon-to-meson ratios are presented in Figure 7. Data for Ξ^-/π^+ and Λ^0/π^+ were calculated along the lower green and blue curves of the phase diagram (right panel in Figure 6), which correspond to $T^\mathrm{bar}_\mathrm{dec}$ until 0.373 GeV for Ξ^- and 0.27 GeV for Λ, and then along the dash-dotted vertical lines, which are now considered "freezeout lines" at high chemical potentials. Both ratios demonstrate the peak-like behaviour.

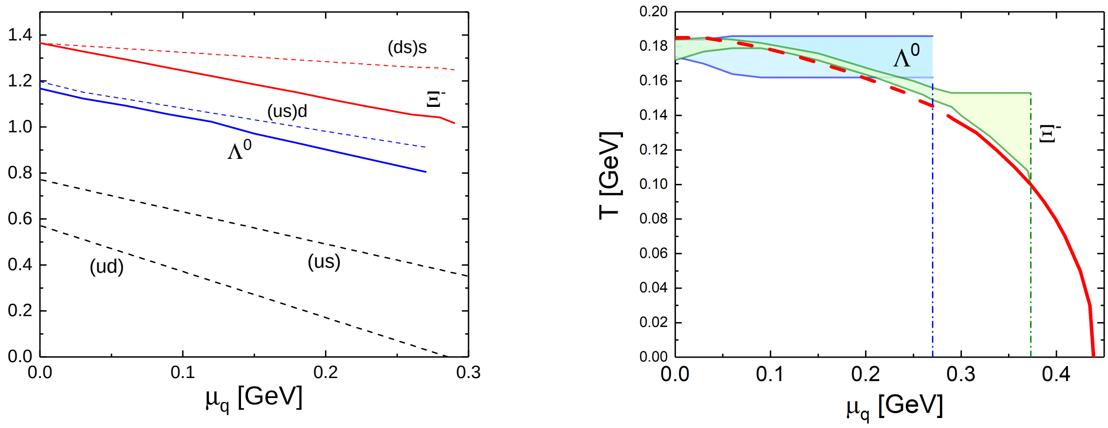

Figure 6. (**left**) Masses of diquarks, baryons, and their threshold $M_D + m_q$ as functions of μ_q. (**right**) Phase diagram of the EPNJL model (red line). The shaded areas show the borders $\{T^{\text{bar}}_{\text{dec}}, T_{\text{diss}}\}$ for baryons, with light blue for Λ and light green for Ξ.

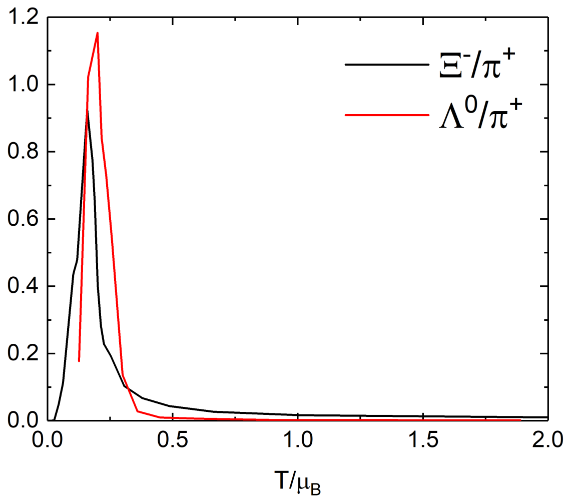

Figure 7. Λ^0/π^+ (red line) and Ξ^-/π^+ (black line) ratios as functions of T$/\mu_B$.

5. Conclusions

This article summarises our calculations of the ratios of mesons and baryons with strangeness to non-strange mesons within the framework of the PNJL-like models. The interest in these ratios is due to them having the "horn" structure in their energy dependencies, which is supposed to be a signal of deconfinement and may be sensitive to the structure of the phase diagram, including the position of CEP and TCP [23]. Our works show that the K^+/π^+ ratio is more sensitive to the matter properties than to the phase diagram structure. This work demonstrates that the EPNJL model reproduces the peak-like structure for the Λ^0/π^+ and Ξ^-/π^+ ratios, but the validity of this estimation is limited by some features of the description of baryons in the model. Therefore, most of our analysis must primarily be taken as qualitative hints (e.g., about the role of the strange quark chemical potential and pion chemical potential or the effect of the vector interaction).

This work addresses several aspects related to the description of baryons as diquark-quark bounded states. The first one is associated with the selection of correct model parameters, which would make it possible to obtain proton and other baryon masses below the threshold value $M_D + mq$. For example, our parameters and choice of the model variation affected the deconfinement temperatures of the baryons. The statistical model and the experiment predicted a lower chemical freeze-out temperature for protons in comparison with that for Ξ. This difference was about 30 MeV [20,24]. The PNJL model with our parameters showed 20 MeV, while the EPNJL model showed 10 MeV.

The second aspect is related to the description of the baryon as a diquark-quark state in the framework of the (E)PNJL model. As noted above, this model usually takes into account only the scalar part in the mass equations (Equations (13)–(16)), skipping the axial-vector part. Nevertheless, in [25,26], it was shown that the accounting for the axial-vector part in mass equations plays an important role in the correct description of the baryon properties [26].

The third aspect concerns the description of baryons as a quark-diquark state at a high chemical potential. At a low density, the two-quark pair forms tightly bound localised diquark states, which can pick up another quark with the right colour to form a colour-singlet baryon. The rise in the chemical potential (or density) leads to a weakening of the interaction strength between quarks and forms weakly bounded Cooper pairs in an attractive colour anti-triplet channel, leading to the phenomenon of colour superconductivity. However, in dense matter, the diquark does not have to be stable in order to form a stable baryon, since it can be a bounded state of three quarks, or the so-called Borromean state [15,21].

In this situation, further improvements on the more fundamental side, allowing one to include the axial-vector part and describe the baryon above critical densities, are highly desirable.

Author Contributions: Conceptualization, A.F.; methodology, Y.K.; software, A.F.; formal analysis, A.F.; investigation, A.F. and Y.K.; writing—original draft, A.F.; writing—review & editing, Y.K.; visualization, A.F.; supervision, Y.K. All authors have read and agreed to the published version of the manuscript.

Funding: This research received no external funding.

Data Availability Statement: The data are available upon reasonable request.

Acknowledgments: We acknowledge a discussion with D. Blaschke about the baryon description in the frame of the model. We thank A. Radzhabov for his comments on the quasi-chemical potential for pions and strange chemical potential in nonequilibrium systems.

Conflicts of Interest: The authors declare no conflict of interest.

References

1. Friesen, A.V.; Kalinovsky, Y.L.; Toneev, V.D. Role of the Chiral Phase Transition in Modelling the Kaon-to-Pion Ratio. *JETP Lett.* **2020**, *111*, 129–134.
2. Blaschke, D.; Friesen, A.V.; Kalinovsky, Y.L.; Radzhabov, A.E. Mott Dissociation and Kaon to Pion Ratio in the EPNJL Model. *Phys. Part. Nucl.* **2021**, *52*, 609–614.
3. Blaschke, D.; Friesen, A.V.; Kalinovsky, Y.L.; Radzhabov, A. Chiral phase transition and kaon-to-pion ratios in the entanglement SU(3) PNJL model. *Eur. Phys. J. ST* **2020**, *229*, 3517–3536.
4. Friesen, A.V.; Kalinovsky, Y.L.; Toneev, V.D. Vector interaction effect on thermodynamics and phase structure of QCD matter. *Int. J. Mod. Phys. A* **2015**, *30*, 1550089.
5. Afanasiev, S.V.; Anticic, T.; Barna, D.; Bartke, J.; Barton, R.A.; Behler, M.; Betev, L.; Białkowska, H.; Billmeier, A.; Blume, C.; et al. Energy dependence of pion and kaon production in central Pb + Pb collisions. *Phys. Rev. C* **2002**, *66*, 054902.
6. Andronic, A.; Braun-Munzinger, P.; Stachel, J. Thermal hadron production in relativistic nuclear collisions: The Hadron mass spectrum, the horn, and the QCD phase transition. *Phys. Lett. B* **2009**, *673*, 142–145; Erratum in: *Phys. Lett. B* **2009**, *678*, 516. [CrossRef]
7. Palmese, A.; Cassing, W.; Seifert, E.; Steinert, T.; Moreau, P.; Bratkovskaya, E.L. Chiral symmetry restoration in heavy-ion collisions at intermediate energies. *Phys. Rev. C* **2016**, *94*, 044912.
8. Gazdzicki, M.; Gorenstein, M.I. On the early stage of nucleus-nucleus collisions. *Acta Phys. Polon. B* **1999**, *30*, 2705.
9. Cohen, T.D.; Furnstahl, R.J.; Griegel, D.K. Quark and gluon condensates in nuclear matter. *Phys. Rev. C* **1992**, *45*, 1881–1893. [CrossRef]
10. Nayak, J.K.; Banik, S.; Alam, J.E. The horn in the kaon to pion ratio. *Phys. Rev. C* **2010**, *82*, 024914.
11. Lewicki, M.P.; Turko, L. NA61/SHINE shining more light on the onset of deconfinement. *arXiv* **2020**, arXiv:2002.00631.
12. Oeschler, H.; Cleymans, J.; Hippolyte, B.; Redlich, K.; Sharma, N. Ratios of strange hadrons to pions in collisions of large and small nuclei. *Eur. Phys. J. C* **2017**, *77*, 584. [CrossRef]

13. Buck, A.; Alkofer, R.; Reinhardt, H. Baryons as bound states of diquarks and quarks in the Nambu-Jona-Lasinio model. *Phys. Lett. B* **1992**, *286*, 29–35. [CrossRef]
14. Ebert, D.; Feldmann, T.; Kettner, C.; Reinhardt, H. Heavy baryons in the quark-diquark picture. *Int. J. Mod. Phys. A* **1998**, *13*, 1091–1113.
15. Blanquier, E. Standard particles in the SU(3) Nambu-Jona-Lasinio model and the Polyakov-NJL model. *J. Phys. G* **2011**, *38*, 105003. [CrossRef]
16. Vogl, U.; Weise, W. The Nambu and Jona Lasinio model: Its implications for hadrons and nuclei. *Prog. Part. Nucl. Phys.* **1991**, *27*, 195–272. [CrossRef]
17. Sugano, J.; Takahashi, J.; Ishii, M.; Kouno, H.; Yahiro, M. Determination of the strength of the vector-type four-quark interaction in the entanglement Polyakov-loop extended Nambu–Jona-Lasinio model. *Phys. Rev. D* **2014**, *90*, 037901.
18. Ratti, C.; Thaler, M.A.; Weise, W. Phases of QCD: Lattice thermodynamics and a field theoretical model. *Phys. Rev. D* **2006**, *73*, 014019.
19. Rehberg, P.; Klevansky, S.P.; Hufner, J. Hadronization in the SU(3) Nambu-Jona-Lasinio model. *Phys. Rev. C* **1996**, *53*, 410–429.
20. Torres-Rincon, J.M.; Sintes, B.; Aichelin, J. Flavor dependence of baryon melting temperature in effective models of QCD. *Phys. Rev. C* **2015**, *91*, 065206.
21. Wang, J.c.; Wang, Q.; Rischke, D.H. Baryon formation and dissociation in dense hadronic and quark matter. *Phys. Lett. B* **2011**, *704*, 347–353.
22. Blaschke, D.; Dubinin, A.S.; Zablocki, D. NJL model approach to diquarks and baryons in quark matter. *arXiv* **2015**, arXiv:1502.03084.
23. Andronic, A.; Blaschke, D.; Braun-Munzinger, P.; Cleymans, J.; Fukushima, K.; McLerran, L.D.; Oeschler, H.; Pisarski, R.D.; Redlich, K.; Sasaki, C.; et al. Hadron Production in Ultra-relativistic Nuclear Collisions: Quarkyonic Matter and a Triple Point in the Phase Diagram of QCD. *Nucl. Phys. A* **2010**, *837*, 65–86.
24. Preghenella, R. Identified-particle production and spectra with the ALICE detector in pp and Pb-Pb collisions at the LHC. *Acta Phys. Polon. B* **2012**, *43*, 555.
25. Barabanov, M.Y.; Bedolla, M.A.; Brooks, W.K.; Cates, G.D.; Chen, C.; Chen, Y.; Cisbani, E.; Ding, M.; Eichmann, G.; Ent, R.; et al. Diquark correlations in hadron physics: Origin, impact and evidence. *Prog. Part. Nucl. Phys.* **2021**, *116*, 103835.
26. Cheng, P.; Serna, F.E.; Yao, Z.Q.; Chen, C.; Cui, Z.F.; Roberts, C.D. Contact interaction analysis of octet baryon axial-vector and pseudoscalar form factors. *Phys. Rev. D* **2022**, *106*, 054031.

Disclaimer/Publisher's Note: The statements, opinions and data contained in all publications are solely those of the individual author(s) and contributor(s) and not of MDPI and/or the editor(s). MDPI and/or the editor(s) disclaim responsibility for any injury to people or property resulting from any ideas, methods, instructions or products referred to in the content.